Theoretical investigations of electronic structure and charge transport properties in polythiophene-based organic field-effect transistors

Article *in* Polymer International · January 2010

DOI: 10.1002/pi.2683

CITATIONS
76

READS
536

3 authors:

Yi-Kang Lan
National Tsing Hua University
33 PUBLICATIONS **945** CITATIONS
SEE PROFILE

Cheng-Han Yang
Academia Sinica
18 PUBLICATIONS **183** CITATIONS
SEE PROFILE

Hsiao-Ching Yang
Fu Jen Catholic University
63 PUBLICATIONS **1,489** CITATIONS
SEE PROFILE

Mini-review

Received: 6 January 2009 Revised: 8 May 2009 Accepted: 8 May 2009 Published online in Wiley Interscience: 30 September 2009

(www.interscience.wiley.com) DOI 10.1002/pi.2683

Theoretical investigations of electronic structure and charge transport properties in polythiophene-based organic field-effect transistors

Yi-Kang Lan, Cheng Han Yang and Hsiao-Ching Yang*

Abstract

Regioregular poly(3-hexylthiophene) (P3HT) is a hole transport polymer material used in organic field-effect transistors (OFETs) and can reach mobilities as high as 0.1 $cm^2\ V^{-1}\ s^{-1}$. Factors that affect the charge mobility and the transport mechanisms of P3HT-based OFET systems are therefore of great importance. We use quantum mechanical methods to interpret the charge mobility and the transport properties of self-assembled P3HT molecules along the intra-chain and inter-chain directions. Our approach is illustrated by a hopping transport model, in which we examine the variation of charge mobility with torsional angle and the intermolecular distance between two adjacent thiophene segments. We also simulate packed P3HT structures via molecular dynamics (MD) simulations. The MD results indicate that the resultant mobility along the $\pi - \pi$ inter-chain direction is significantly less than that along the intra-chain direction. Accordingly, the main charge-transfer route within the P3HT ordered domains is an intra-chain rather than an inter-chain one. The calculation result for the inter-chain hole mobility is around $10^{-2}\ cm^2\ V^{-1}\ s^{-1}$, which is consistent with experimental data from P3HT single fibril.

Keywords: charge transport; transfer integral; charge mobility; P3HT; organic thin-film transistor; OTFT

INTRODUCTION

Polymer electronics is a branch of organic electronics that deals with conductive polymers. Compared to small molecules, polymer electronics based on conductive polymers are lighter, more flexible and can be manufactured relatively easily with the printing process. Amongst several polymer-based electronic devices, the main control unit is the transistor which amplifies or switches the electronic signals in integrated circuits. In polymer electronics, transistors can be made using conducting polymers due to the semiconductor characteristics. They are known as organic field-effect transistors (OFETs) or organic thin-film transistors. They have been applied in many electronic devices such as large-area thin sensors, electronic paper and active matrix displays.[1–3] An OFET operates as a capacitor where the transport layer is a conducting channel between two ohmic contacts, the source and drain electrodes. The density of charge carriers in the conducting channel is modulated by the voltage applied to the second plate of the gate electrode. Accordingly, the efficiency of an OFET device is mainly determined by the transport layer (the semiconductor layer). Thus, enhancing the charge mobility of OFETs to the range of *ca* 10 $cm^2\ V^{-1}\ s^{-1}$, as is the case in a-Si : H FETs, is the key issue of this field. The regioregular poly(3-hexylthiophene) (rr-P3HT) system can reach mobilities as high as 0.1 $cm^2\ V^{-1}\ s^{-1}$ throughout the polymer-based transport layer. Thus, to clarify the factors that affect the charge-transport mechanisms of the P3HT system is of great importance.

One of the most fascinating physical properties of the rr-P3HTs is their ordered packing structures. Experimental data suggest that rr-P3HT can form self-assembled lamellar structures.[4–6] In the ordered packing P3HT systems, the key factors that affect the charge mobility are the molecular regioregularity, molecular weight, temperature and processing conditions. Sirringhaus *et al*. reported that self-assembled P3HT lamellae in FETs can adopt two different orientations with respect to the substrate by tuning the molecular regularity and processing conditions. A significant increase in the charge mobility can be achieved by varying the orientation of the ordered lamellae from parallel to perpendicular with respect to the substrate. This result may lead to the conclusion that the charge transport along the $\pi - \pi$ stacking inter-chains plays a dominant role in the high carrier mobility of rr-P3HT in FETs.[7] However, it should be noted that varying the P3HT molecular regioregularity not only results in different packing orientations of the lamellae (i.e. dimensionality of the charge-transfer route) but also strongly affects the chain conformation and chain packing. A few studies have shown that increasing the molecular regularity can lead to an extended π-conjugation as well as more dense packing of chains along the $\pi - \pi$ stacking direction.[8–14] For example, McCullough *et al*. employed molecular mechanics and *ab initio* calculations to examine the

* *Correspondence to: Hsiao-Ching Yang, 510 Chung Cheng Road, Hsinchuang, Taipei County 24205, Taiwan, Republic of China.*
E-mail: 068204@mail.fju.edu.tw

Department of Chemistry, Fu Jen Catholic University, Hsinchuang, Taipei 24205, Taiwan

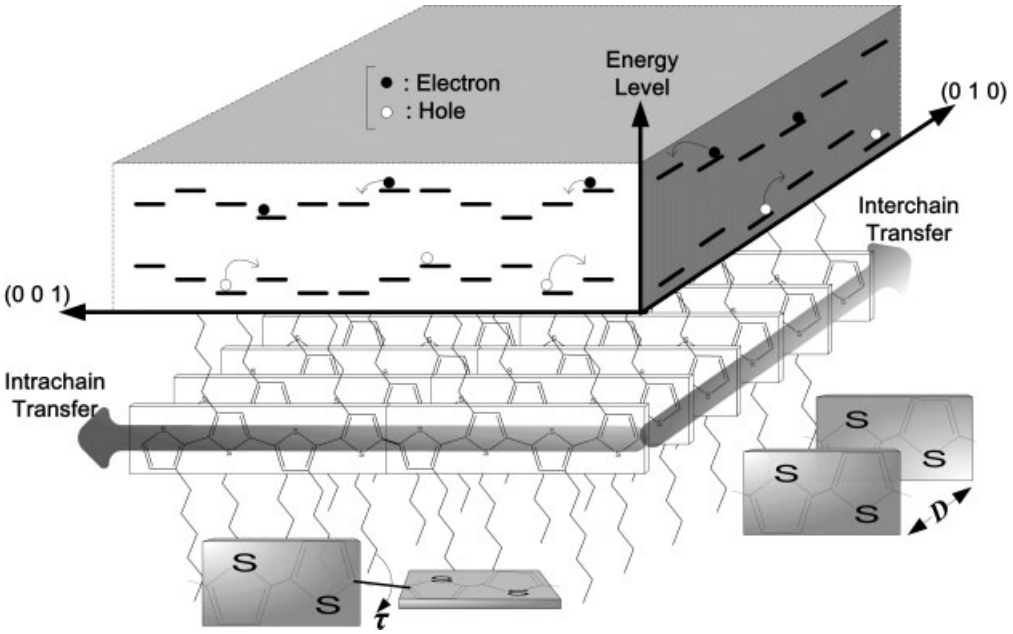

Figure 1. Schematic of the two-state hopping model along the intra-chain and inter-chain directions. The variables τ and D are indicated.

conformation of P3HT with different head-to-tail and head-to-head configurations.[11] They observed that the existence of head-to-head coupling causes the torsion angle to deviate significantly out of the plane. The conjugation length can be effectively shortened through ring rotation. Accordingly, one cannot exclude the possibility that the more coil-like chain conformation (by decreasing P3HT regularity) will significantly reduce the charge transport along the intra-chain direction. Also, P3HT nanofibril experiments suggest that the charge mobility along the pure $\pi - \pi$ stacking directions is in the range 0.02–0.06 $cm^2\ V^{-1}\ s^{-1}$. Thus the addition of an extra transport path through the $\pi - \pi$ stacking directions may not be sufficient to improve the mobility to 0.1 $cm^2\ V^{-1}\ s^{-1}$.

As stated above, despite experimental studies that have addressed how the charge mobility is influenced, the issue of whether the high carrier mobility of ordered rr-P3HT is mainly attributed to inter-chain or intra-chain charge transfer still remains unconfirmed. The details of the transport model around the packing structures for different transport routes need to be clarified. In this research, we thus aim to examine theoretically how intra-chain and inter-chain charge-transport properties are affected by the chain conformation and chain packing within the ordered lamellar region.

THEORETICAL METHODS AND SYSTEM

In this research, we adopted a hopping model to describe the charge-transport properties along both the intra-chain and inter-chain directions in the P3HT system. At room temperature, the motion of the carriers can be described as a sequence of uncorrelated hopping processes, as shown in Fig. 1. In particular, we artificially varied the torsional angle τ between two conjugated thiophene segments along the main chain to resemble the local deformation created by the molecular regularity and/or temperature, and calculated the charge mobility values as a function of τ. Each segment contains two thiophene rings in a *trans* conformation. In analyzing the charge-transport properties along the $\pi - \pi$ stacking inter-chains, we considered two segments separated by a distance D. By varying the intermolecular distance D, we investigated the influence of molecular packing on the hole mobility along the inter-chains.

The relationship between the carrier mobility μ and the charge-transfer rate (hopping probability per unit time) k_{CT} can be expressed as[15,16]

$$\mu = \frac{ea^2}{2k_BT}k_{CT} \tag{1}$$

where k_B, T, a and e are the Boltzmann constant, temperature, transport distance and electronic charge, respectively. The transport distance a can be obtained via a quantum mechanical geometry optimized structure.

To obtain the charge-transfer rate, we can introduce the semi-classical Marcus theory. The Marcus theory was originally developed by Rudolph A Marcus to explain the rates of electron-transfer reactions – the rate at which an electron can move or hop from one chemical species (called the electron donor) to another (called the electron acceptor).[17,18] According to the semi-classical Marcus theory, the charge-transfer rate k_{CT} between neighboring segments can be expressed as follows:[19,20]

$$k_{CT} = \frac{2\pi}{\hbar^2}t^2\sqrt{\frac{1}{4\lambda\pi k_BT}}\exp\left[\frac{-(\Delta G^\circ + \lambda)^2}{4\lambda k_BT}\right] \tag{2}$$

where $\hbar$, t and λ are Planck's constant, the transfer integral and the inner reorganization energy, respectively. ΔG° is the difference between the Gibbs free energy of the system before and after the charge-hopping process and is equal to zero since the segments are identical. Thus, we need to determine the magnitude of the transfer integral t and reorganization energy λ to find the charge transfer rate k_{CT} and the charge mobility μ.

The inner reorganization energy comes from the vibrational structure change due to the electron gain/loss process of the segment. We here use E_{neu} and E^+_{ion} to denote the energy of the

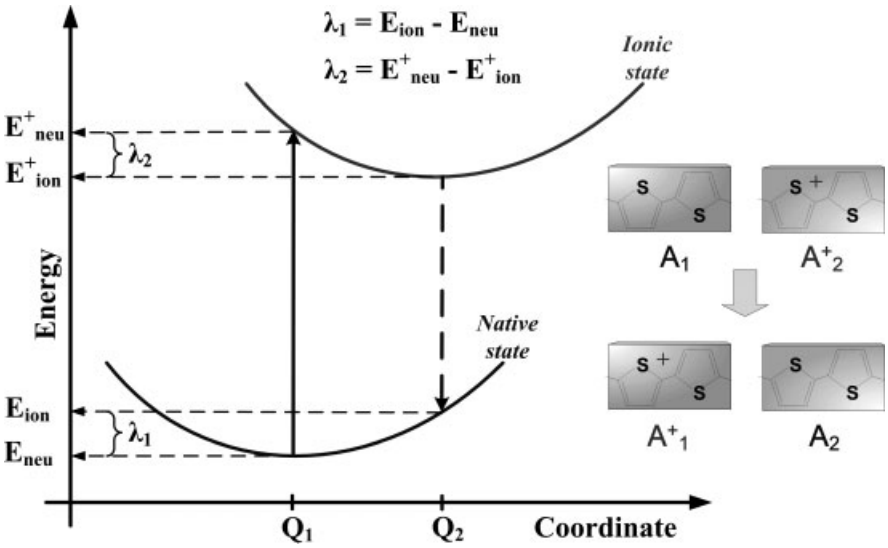

Figure 2. Schematic of the reorganization energy *versus* the reaction coordinate. The upper and lower curves denote the ionic and neutral states of the segment, respectively.

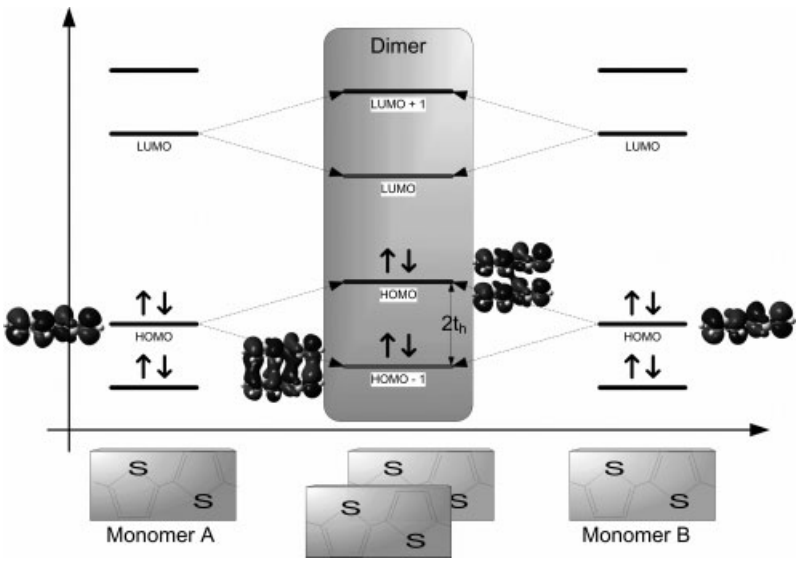

Figure 3. Hybrid orbitals of the interacting dimer. The splitting of the HOMO and HOMO-1 in the dimer is due to the coupling/hybrid of the HOMO of each monomer.

optimized, stable structure of the natural segment and the ionized segment, respectively. Both of them are in the lowest point of the natural and ionized potential curve, respectively. E^{+}_{neu}/E_{ion} denote the energy of the segment that has lost/gained an electron, but still has an unchanged segment structure. Thus, they are located in the same vibrational coordinate compared to the native/ionized segment, but on different potential energy surfaces, as shown in Fig. 2. The axis Q denotes the vibrational coordinate; Q_1 and Q_2 are the equilibrium vibration centers of the neutral and ionized state. The first part, λ_1, arises from the energy difference due to the structural relaxation of gaining an electron, and λ_2 arises from losing an electron. Accordingly, λ_1 can represent the energy difference between E_{neu} and E_{ion}, and λ_2 can represent the energy difference between E^{+}_{neu} and E^{+}_{ion}. The reorganization energy λ can be calculated using

$$\lambda = \lambda_1 + \lambda_2 = (E_{ion} - E_{neu}) + (E^{+}_{neu} - E^{+}_{ion}) \quad (3)$$

All energy states can be obtained with the structure optimization and total energy calculation processes using quantum mechanical methods.

The transfer integral of a given system is related to the energetic splitting of electronic levels, which is attributed to segment interaction. In each of the isolated segments (monomers), the highest occupied molecular orbital (HOMO) is the π-bonding orbital delocalized over the segment with energy ε. When two segments approach each other and the HOMO of each segment starts to interact, a new HOMO and HOMO-1 are formed in the dimer system due to the hybrid of the monomer HOMOs. Thus, the energetic splitting due to the segment interaction is equal to the energy difference between the HOMO and HOMO-1 in the interacting segment pairs, as shown in Fig. 3. The transfer integral t of the hole is thus given by

$$t_{hole} = \frac{1}{2}\sqrt{(E_H - E_{H-1})^2 - (\varepsilon_1 - \varepsilon_2)^2} \quad (4)$$

where E_H and E_{H-1} are the energy of HOMO and HOMO-1, respectively. The total energy for each isolated segment is equal, that is, $\varepsilon_1 = \varepsilon_2$ in our case, and so Eqn (4) becomes

$$t_{hole} = \frac{E_H - E_{H-1}}{2} \quad (5)$$

The theoretical model presented above has been used successfully to describe the conductive properties of small-molecule-based organic transistors such as pentacene systems.[21,22]

All of the above electronic energy levels and geometry optimizations were carried out using the mp2/6-311G (d,p) quantum mechanical simulations. The mp2 (Møller–Plesset second-order perturbation theory) is based on the Hartree–Fock method but includes electron correlation terms. Hence, it is suitable to describe the long-range interactions of organic molecular pairs such as $\pi - \pi$ interactions.[23]

We also employed molecular dynamics (MD) with a PCFF (polymer consistent force field)[24] to simulate the equilibrated P3HT structures at regularity equal to 100% and room temperature in a given packing state. In the simulation of the packing state, the system contains 4 P3HT molecules with 64 thiophene rings per chain and each P3HT molecule is artificially set as an infinite chain[25] to avoid the influence of the end group libration. Initially, the 4 P3HT molecules were set to form a lamellar structure with an inter-chain separation distance of 4.0 and 17 Å along the $\pi - \pi$ stacking and side-chain packing directions, respectively. The packed state simulations were carried out in the isothermal–isobaric ensemble (NPT) with a time step of 1 fs, and the system temperature and pressure were set to 300 K and 10^{-4} GPa (1 atm), respectively.

RESULTS AND DISCUSSION

Figure 4 shows the four calculated energy levels of HOMO-1, HOMO, lowest unoccupied molecular orbital (LUMO) and LUMO+1 for two conjugated thiophene segments as a function of the torsional angle τ. From these calculated electronic structures, we obtained the transfer integral t of a hole along the intra-chains using Eqn (5), and the transfer integral t can combine with the reorganization energy λ and the transfer distance a to obtain the hole mobility, as shown in Fig. 5. Also, the hole mobility along the inter-chain direction as a function of D can be obtained with similar processes, also shown in Fig. 5. It can be clearly seen that the intra-chain hole mobility has a maximum transfer integral value at $\tau = 180^\circ$, i.e. when the neighboring thiophene rings are in the *trans* conformation. As τ deviates from 180°, the hole mobility decreases progressively to a minimum value of *ca* 10^{-3} when the neighboring thiophenes are located perpendicular to each other ($\tau = 90^\circ$). The calculation results also indicate that the inter-chain hole mobility shows a logarithmic increase with a decrease in the inter-chain distance. This significant increase is mainly due to the fact that the coupling strength of p-orbitals along the intermolecular direction increases with decreasing separation distance. Accordingly, one may expect that a relatively large mobility along the inter-chain direction may be obtained as long as the molecules are close to each other. However, a significantly large repulsive force is often accompanied very tightly packed structures.[26] Results are shown for an average distance of *ca* 3.8 Å between the intermolecular layers.

So far, we have discussed the effects of the local degree of distortion of the thiophene rings and the intermolecular distance on the intra-chain and inter-chain hole mobility. The remaining issue is how the torsional angle of the backbone rings and the inter-chain packing are influenced by the surroundings, including the neighboring chains and thermal fluctuations. To illustrate these effects, we employed a MD simulation method to obtain the energy-minimized molecular structure of 4 P3HT molecules with 64 thiophene rings per chain, regularity values of 100% and a temperature of 300 K. Figure 6 shows the simulated molecular structures at 300 K with regularity of 100%. The MD results indicate that the packing structures of the P3HT side chains may mix with both random conformations and the zigzag packing forms. According to these average structure conformations, the related charge-transfer rate and charge mobility via Fig. 5 are given in Table 1.

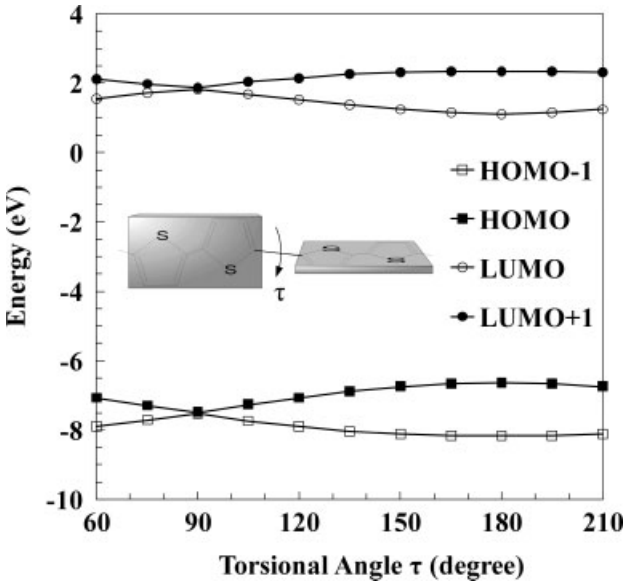

Figure 4. Calculated energy levels of HOMO-1, HOMO, LUMO and LUMO+1 as a function of the torsional angle τ of the two conjugated segments.

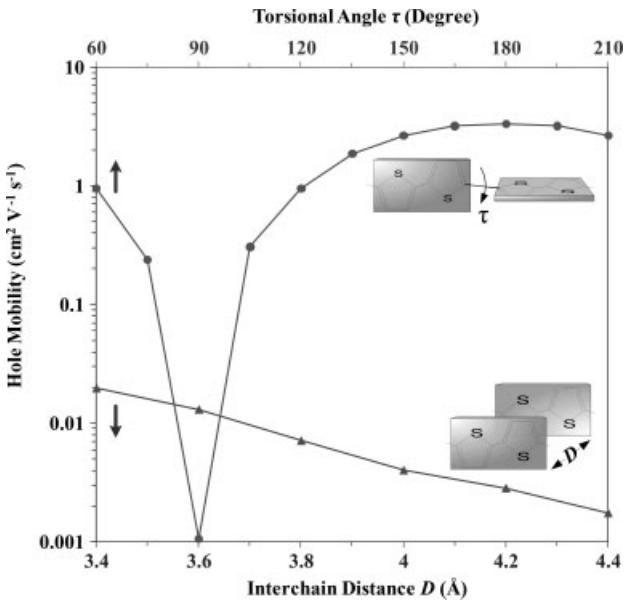

Figure 5. Intra-chain hole mobility as a function of the torsional angle τ of the conjugated segments (●) and the inter-chain hole mobility as a function of the intermolecular separation distance D (▲).

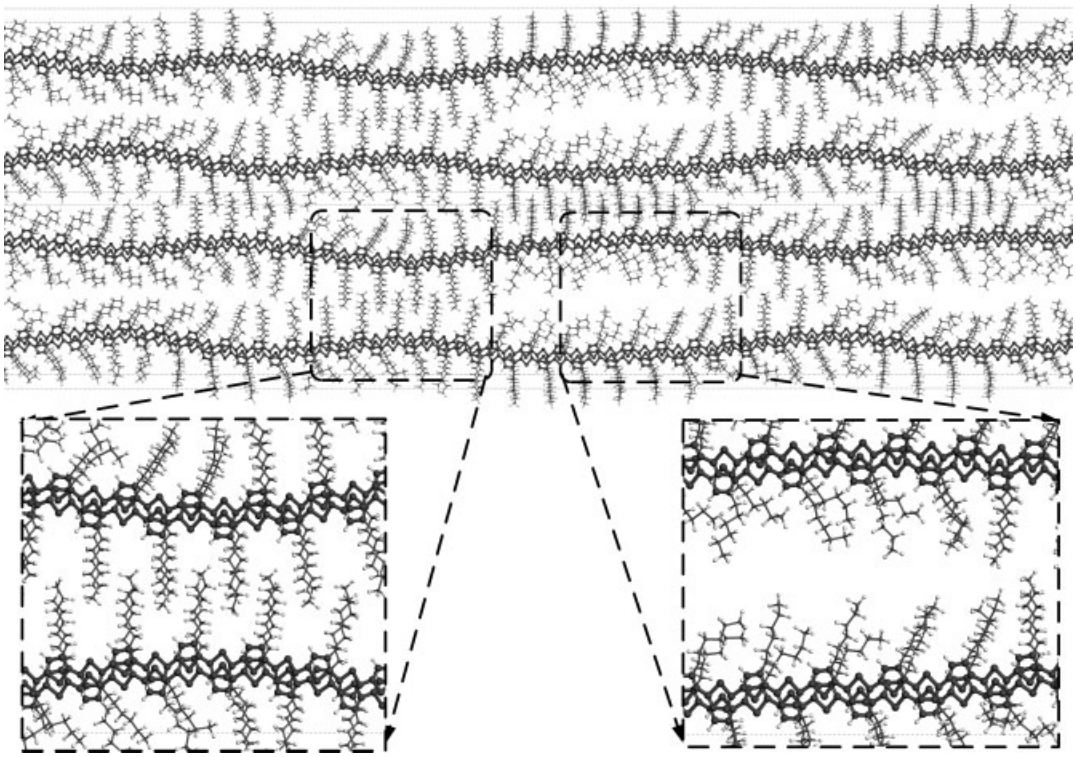

Figure 6. MD result illustrates the equilibrium structures of the 100% regioregular P3HT system at 300 K.

Table 1. Charge-transfer rate and hole mobility along the inter-chain and intra-chain directions within the characteristic structure

Transport direction	Structure information	Transfer rate (s^{-1})	Mobility ($cm^2\ V^{-1}\ s^{-1}$)
Intra-chain	180°[a]	1.62×10^{13}	3.34
Inter-chain	3.8 Å[b]	2.54×10^{11}	7.13×10^{-3}

[a] Torsional angle τ.
[b] The $\pi - \pi$ distance D between thiophene segments.

The results suggest that in the ordered region, the hole mobility along the intra-chain direction is about two orders of magnitude greater than it is along the inter-chain direction. The large difference in the charge-transfer rate suggests that the charge will mainly pass though the main chain instead of transport occurring via inter-chain $\pi - \pi$ coupling. This means that the main transfer route in the ordered region is along the polymer chain. In addition, the large repulsion and the $\pi - \pi$ attraction result in an inter-chain distance of around 3.8 Å, and the inter-chain mobility is limited to about 10^{-2} $cm^2\ V^{-1}\ s^{-1}$. This calculation result is consistent with OFET experiments using P3HT single fibers as the transport layer, whose effective charge-transfer route is through the $\pi - \pi$ direction.[27] The mobility measured in the single-fiber experiments is around 10^{-2} $cm^2\ V^{-1}\ s^{-1}$.[28,29]

CONCLUSIONS

We employed MD and quantum mechanics to examine the molecular conformation and the charge-transport properties of P3HT molecules in ordered states, and calculate the hole mobility. In particular, we adopted a hopping transport model and focused on the effects of the chain conformation and chain structure on the anisotropic transfer routes, i.e. the intra-chain and inter-chain directions, of the ordered zones. We found that in the well-packed P3HT lamellae, the charge-transfer rate along the main chain is larger than it is along the $\pi - \pi$ inter-chain by two orders of magnitude. Accordingly, we conclude that the main dominating charge-transport route within the P3HT ordered domains is along the intra-chain rather than the inter-chain direction.

ACKNOWLEDGEMENT

This work was supported by the National Science Council of the Republic of China through grant NSC 97-2113-M-030-002-MY2.

REFERENCES

1 Reese C, Roberts M, Ling M and Bao Z, *Mater Today* Sept.: **20**:(2004).
2 Klauk H (ed.), *Organic Electronics: Materials, Manufacturing and Applications*. Wiley-VCH, Weinheim (2006).
3 Gamota D, Brazis P, Kalyanasundaram K and Zhang J (eds), *Printed Organic and Molecular Electronics*. Kluwer Academic, Boston, MA (2004).
4 McCullough RD, Tristramnagle S, Williams SP, Lowe RD and Jayaraman M, *J Am Chem Soc* **115**:4910 (1993).
5 Prosa TJ, Winokur MJ and McCullough RD, *Macromolecules* **29**:3654 (1996).
6 McCullough RD, *Adv Mater* **10**:93 (1998).
7 Sirringhaus H, Brown PJ, Friend RH, Nielsen MM, Bechgaard K, Langeveld-Voss BMW, *et al*, *Synth Met* **111**:129 (2000).
8 Chen TA, Wu XM and Rieke RD, *J Am Chem Soc* **117**:233 (1995).
9 Kaneto K, Hatae K, Nagamatsu S, Takashima W, Pandey SS, Endo K, *et al*, *Jpn J Appl Phys Part 2 Lett* **38**:L1188 (1999).
10 Kim Y, Cook S, Tuladhar SM, Choulis SA, Nelson J, Durrant JR, *et al*, *Nature Mater* **5**:197 (2006).
11 McCullough RD, Lowe RD, Jayaraman M and Anderson DL, *J Org Chem* **58**:904 (1993).

12 McCullough RD, Lowe RD, Jayaraman M, Ewbank PC, Anderson DL and Tristramnagle S, *Synth Met* **55**:1198 (1993).
13 Pandey SS, Takashima W, Nagamatsu S, Endo T, Rikukawa M and Kaneto K, *Jpn J Appl Phys Part 2 Lett* **39**:L94 (2000).
14 Sentein C, Mouanda B, Rosilio A and Rosilio C, *Synth Met* **83**:27 (1996).
15 Deng WQ and Goddard WA, *J Phys Chem B* **108**:8614 (2004).
16 Coropceanu V, Cornil J, da Silva DA, Olivier Y, Silbey R and Bredas JL, *Chem Rev* **107**:926 (2007).
17 Marcus RA, *Annu Rev Phys Chem* **15**:155 (1964).
18 Marcus RA, *Angew Chem Int Ed Engl* **32**:1111 (1993).
19 Liang CX and Newton MD, *J Phys Chem* **96**:2855 (1992).
20 Bredas JL, Beljonne D, Coropceanu V and Cornil J, *Chem Rev* **104**:4971 (2004).
21 Kwon O, Coropceanu V, Gruhn NE, Durivage JC, Laquindanum JG, Katz HE, *et al*, *J Chem Phys* **120**:8186 (2004).
22 Chen HY and Chao I, *Chem Phys Lett* **401**:539 (2005).
23 Tsuzuki S, Honda K and Azumi R, *J Am Chem Soc* **124**:12200 (2002).
24 Sun H, *Macromolecules* **28**:701 (1995).
25 Yang HC, Hu CY, Ku MY, Huang Q and Chen CL, *ChemPhysChem* **5**:373 (2004).
26 Lan YK and Huang CI, *J Phys Chem B* **112**:14857 (2008).
27 Kim DH, Jang Y, Park YD and Cho K, *J Phys Chem B* **110**:15763 (2006).
28 Merlo JA and Frisbie CD, *J Polym Sci B: Polym Phys* **41**:2674 (2003).
29 Merlo JA and Frisbie CD, *J Phys Chem B* **108**:19169 (2004).

